LATERAL MOBILITY IN MEMBRANES AS DETECTED BY FLUORESCENCE RECOVERY AFTER PHOTOBLEACHING

JUAN YGUERABIDE, JEFFREY A. SCHMIDT, AND EVANGELINA E. YGUERABIDE
Department of Biology, University of California, San Diego, La Jolla, California 92093

ABSTRACT The evaluation of lateral diffusion coefficients of membrane components by the technique of fluorescence recovery after photobleaching (FRAP) is often complicated by uncertainties in the values of the intensities $F(0)$, immediately after bleaching, and $F(\infty)$, after full recovery. These uncertainties arise from instrumental settling time immediately after bleaching and from cell, tissue, microscope, or laser beam movements at the long times required to measure $F(\infty)$. We have developed a method for precise analysis of FRAP data that minimizes these problems. The method is based on the observation that a plot of the reciprocal function $R(t) = F(\infty)/[F(\infty)-F(t)]$ is linear over a large time range when (*a*) the laser beam has a Gaussian profile, (*b*) recovery involves a single diffusion coefficient, and (*c*) there is no membrane flow. Moreover, the ratio of intercept to slope of the linear plot is equal to $t_{1/2}$, the time required for the bleached fluorescence to rise to 50% of the full recovery value, $F(\infty)$. The lateral diffusion coefficient D is related to $t_{1/2}$ by $t_{1/2} = \beta w^2/4D$ where β is a defined parameter and w is the effective radius of the focused laser beam. These results are shown to indicate that the recovery of fluorescence $F(t)$ can be represented over a large range of percent bleach, and recovery time t by the relatively simple expression $F(t) = [F(0) + F(\infty)\,(t/t_{1/2})]/[1 + t/t_{1/2})]$. FRAP data can therefore be easily evaluated by a nonlinear regression analysis with this equation or by a linear fit to the reciprocal function $R(t)$. It is shown that any error in $F(\infty)$ can be easily detected in a plot of $R(t)$ vs. t which deviates significantly from a straight line when $F(\infty)$ is in error by as little as 5%. A scheme for evaluating D by linear analysis is presented. It is also shown that the linear reciprocal plot provides a simple method for detecting flow or multiple diffusion coefficients and for establishing conditions (data precision, differences in multiple diffusion coefficients, magnitude of flow rate compared to lateral diffusion) under which flow or multiple diffusion coefficients can be detected. These aspects are discussed in some detail.

INTRODUCTION

The technique of fluorescence recovery after photobleaching, FRAP, (1–8) has been used to study the lateral mobility of membrane lipids and proteins in a variety of cells and tissues. Cell systems studied in our laboratory include lymphocytes (9), developing muscle cells (10), kidney cultured cells (11), photoreceptors,[1] and vasopressin-sensitive tissue.[1] In these studies we have found that analysis of FRAP data is often limited by difficulties in the evaluation of the fluorescence intensity $F(0)$ immediately after photobleaching and the intensity $F(\infty)$ after full recovery at long times. Uncertainties in the values of these intensities due to instrumental fluctuations and cell or tissue movements can introduce large errors in the values of diffusion coefficients evaluated from FRAP data.

In our investigations of these problems, we developed a method for linearizing FRAP data which has proved useful in evaluating and minimizing possible errors in analysis. In this paper we present the details of the method and exemplify its applicability with data from very thin multibilayer films. Applications to living cells are reported elsewhere.

THEORY OF FRAP EXPERIMENTS

In a FRAP experiment, an attenuated laser beam is focused on a small area of a membrane that is uniformly labeled with a fluorescent lipid or protein probe, and the fluorescence intensity excited by the beam is monitored as a function of time. At a predetermined time, the optical attenuator is momentarily removed for a fraction of a second to bleach some of the probe molecules in the illuminated area. The fluorescence intensity is reduced by the bleaching pulse but the intensity subsequently recovers through diffusion of unbleached molecules from the surrounding, unilluminated area. The lateral diffusion coefficient of the labeled molecules is evaluated by analysis of the recovery graph.

For the case where the laser beam has a Gaussian profile and recovery occurs only by diffusion, the recovery of fluorescence intensity $F(t)$ is given (1, 5) by the expression

$$F(t) = F^{\circ}\sum_{n=0}^{\infty}[(-K)^n/n!]\,[1 + n\,(1 + 2t/\tau_D)]^{-1} \qquad (1)$$

where the characteristic diffusion time τ_D is defined by the expression

$$\tau_D = w^2/4D. \qquad (2)$$

D is the lateral diffusion coefficient of the fluorescent labeled molecules, w is the half-width at $1/e$ height of the laser beam at its point of focus on

[1] Yguerabide, J., M. C. Foster, J. A. Schmidt, and E. E. Yguerabide. Manuscript in preparation.

the membrane, F^0 is the fluorescence intensity before bleaching, and K is a parameter related to the fraction P of fluorophore bleached. P is defined as

$$P = \frac{F^0 - F(0)}{F^0} \tag{3}$$

where $F(0)$ is the fluorescence intensity immediately after bleaching. More explicitly, for any percent bleach, the value of K can be calculated with the expression

$$[F(0)]/F^0 = K^{-1}(1 - e^{-K}). \tag{4}$$

Eq. 1 can also be used to describe the recovery of fluorescence intensity when there is incomplete recovery, i.e., $F(\infty) \neq F^0$. More explicitly, for the case where the fraction of the fluorescence intensity that does recover is determined by a single diffusion coefficient, we can write,

$$F(t) = \left\{\frac{f(t) - [F_1(0)/F_1^0]}{1 - [F_1(0)/F_1^0]}\right\}[F(\infty) - F(0)] + F(0) \tag{5}$$

where

$$f(t) = \sum_{n=0}^{\infty} [(-K)^n/n!]\,[1 + n(1 + 2t/\tau_D)]^{-1}. \tag{6}$$

$F(t)$, $F(0)$, and $F(\infty)$ refer to total intensities whereas F_1^0 and $F_1(0)$ refer to that part of the fluorescence intensity contributed by the diffusing species responsible for recovery, i.e., $F_1(0)/F_1^0$ is the fraction of the diffusing species that is bleached. It should be noted that the term in brackets in Eq. 5 gives the fraction of recoverable fluorescence that is recovered at any time t, the term $F(\infty) - F(0)$ gives the amplitude of the recovery and $F(0)$ gives the starting intensity for the recovery. If all species have the same bleaching characteristics, i.e., same extinction coefficient and bleaching efficiency, than $F_1(0)/F_1^0 = F(0)/F^0$ where $F(0)$ and F^0 are total intensities.

In the evaluation of FRAP data it is often convenient to plot results as normalized fractional recovery $\bar{F}(t)$ vs. t where $\bar{F}(t)$ is defined as

$$\bar{F}(t) = [F(t) - F(0)]/[F(\infty) - F(0)]. \tag{7}$$

The time $t_{1/2}$ required to recover half of the bleached intensity, i.e., the time required for $\bar{F}(t)$ to rise from $\bar{F} = 0$ to $\bar{F} = 0.5$, is related to τ_D and the diffusion coefficient by the expression

$$t_{1/2} = \beta\,\tau_D = \frac{\beta w^2}{4D}. \tag{8}$$

β is a parameter which depends on the percent bleach P and takes into consideration the fact that the effective "spot size" of the bleached area for a Gaussian beam depends on the percent bleached. The value of β for a given value of P can be evaluated numerically from a theoretical plot of F vs. t/τ_D generated as described below and shown in Table I.

For the case where recovery of fluorescence is due both to diffusion and uniform membrane flow or cell movement, the recovery of fluorescence intensity is given, for a bleaching beam with Gaussian profile, by the expression (5)

$$F(t) = F^0 \sum_{n=0}^{\infty} \frac{(-K)^n \exp\{-2(t/\tau_F)^2 n/[1 + n(1 + 2t/\tau_D)]\}}{n!\,[1 + n(1 + 2t/\tau_D)]} \tag{9}$$

where τ_F is the characteristic recovery time for flow and is defined as:

$$\tau_F = w/V_0 \tag{10}$$

V_0 is the velocity for the uniform flow and w, τ_D, and K are as previously defined. When fluorescence recovery is completely dominated by flow (i.e., $D = 0$), then $t_{1/2}$ for recovery is given by

$$t_{1/2} = \frac{\beta_F w}{V_0} \tag{11}$$

β_F has a value close to 0.9 in the range 0 to 70% bleach (5).

TABLE I
VALUES OF K AND β FOR DIFFERENT VALUES OF PERCENT BLEACH*

Percent bleach	K	β
0	0	1.00
5	0.100	1.00
10	0.225	1.01
15	0.340	1.03
20	0.475	1.04
25	0.610	1.06
30	0.765	1.075
35	0.935	1.09
40	1.14	1.11
45	1.35	1.13
50	1.60	1.15
55	1.88	1.18
60	2.20	1.22
65	2.62	1.26
70	3.20	1.30
80	5.00	1.45
85	6.80	1.59

*As determined from Eq. 4 and numerical analysis of plots of Eq 1.

EVALUATION OF LATERAL DIFFUSION COEFFICIENTS FROM FRAP DATA

The most direct and simplest method for evaluating D from FRAP data is to determine $t_{1/2}$, the time required to go from $F = 0$ to $F = 0.5$, and to evaluate D with Eq. 8. This method, however, depends greatly on the values of $F(0)$ and $F(\infty)$, which are often subject to significant experimental error due to artifacts from instrumental settling, and cell or tissue movements at the long times ($t > 10\ \tau_D$) required to reach $F(\infty)$.

A more accurate method is to curve fit Eq. 1 to the experimental graph of $F(t)$ vs. t, thus making use of all points on the graph. During consideration of curve-fitting methods we arrived at a method for linearizing FRAP data that greatly facilitates the curve-fitting process and minimizes the artifacts mentioned above. Other curve-fitting methods described in the literature are not as precise or general (5, 8) and do not address the problem of uncertainties in $F(0)$ and $F(\infty)$. Our method also allows one to define conditions under which flow and multiple diffusion coefficients can be detected experimentally.

Simple Diffusion, Zero Flow

For low values of percent bleach, consideration of Eq. 1 shows that $F(t)$ can be represented by the function

$$F(t) = \frac{F(0) + F(\infty)(t/t_{1/2})}{1 + (t/t_{1/2})} \tag{12}$$

$$= \frac{F(0) + F(\infty)(t/\beta\tau_D)}{1 + (t/\beta\tau_D)} \qquad (13)$$

with $\beta = 1$. This expression indicates that for low bleach the reciprocal function

$$R(t) = \frac{F(\infty)}{F(\infty) - F(t)} \qquad (14)$$

is a linear function of time. Our linearization procedure is based on the observation that Eqs. 12 and 13 apply even at large percent bleach if the value of β is defined by Eq. 8 and that the ratio intercept/slope of $R(t)$ vs. t obeys the relation

$$\text{intercept/slope} = t_{1/2} = \beta\tau_D. \qquad (15)$$

We established the linearity of the $R(t)$ plots (*a*) by visual inspection of plots calculated with the complete Eq. 1 as shown in Figs. 1 and 2 and (*b*) by least-square fit of each reciprocal plot to a linear function, using weighting functions described below, and calculation of the deviations of the exact values from the straight line values. The largest deviations of course occur at the higher values of percent bleach, but even at 85% bleach the deviations are within experimental errors. Up to 70% bleach, the percent deviations between exact values of $F(t)$ and values calculated from the linear least-square fit of $R(t)$ vs. t are below 1%, and more often below 0.5%, for t/τ_D from zero to at least 10 τ_D. Similarly $t_{1/2}$ values calculated from intercept/slope for different percent bleaches below 70% agree within 1.2% with the exact values. At 85% bleach, a relatively high bleach, the percent deviation between exact and linear least-square values of $F(t)$ are below 4% around $t/\tau_D = 0.5$ and below 1% above $t/\tau_D = 1$ to at least 10 τ_D. More importantly, the $t_{1/2}$ value calculated from intercept/slope at this high bleach agrees within 2% with the exact value. Thus, Eqs. 12–15 give an excellent representation of $F(t)$ and $t_{1/2}$ up to at least 85% bleach. It should be noted that our FRAP experiments are usually done below 70% bleach.

Eqs. 12–15 also apply as written to the case of incomplete recovery as can be seen by introducing Eq. 12 for $F_1^\circ f(t)$ in (5). The exact value of β which applies in this case is the value given in Table I for the overall fractional bleach $[F^\circ - F(0)]/F^\circ$, assuming that all fluorescent species have the same bleaching characteristics.

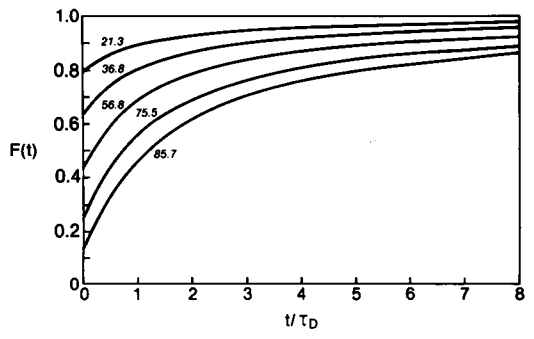

FIGURE 1 Fluorescence recovery graphs for different values of percent bleach. Graphs were calculated with Eq. 1. The number next to each graph refers to percent bleach as defined in Eq. 3. Values of K used in the calculations are shown in Table I.

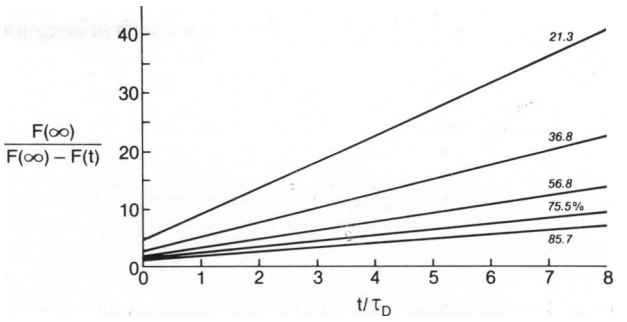

FIGURE 2 Fluorescence recovery graphs of Fig. 1 plotted in terms of the reciprocal function $F(\infty)/[F(\infty) - F(t)]$ vs. t/τ_D. These graphs demonstrate the linearity of the reciprocal plots.

An alternate method for viewing our representation of $F(t)$ by Eq. 13 is obtained by equating Eqs. 1 and 13 and solving for β. These manipulations show that Eq. 13 is an exact representation of $F(t)$ if β is defined by the time-dependent expression

$$\beta(t) = \frac{\sum_{n=1}^{\infty} (-K)^n/\{n![1 + n(1 + 2t/\tau_D)]\}}{\sum_{n=1}^{\infty} [2n/(1+n)](-K)^n/\{n![1 + n(1 + 2t/\tau_D)]\}}. \qquad (16)$$

Our approximate representation, of course, assumes that β is time independent. Numerical calculations indicate that for a given percent bleach in the range 0 to 70%, β, does not vary by >11% over the range $0 \leq t/\tau_D \leq 10$. The method of analysis presented above in terms of reciprocal plots, however, is a more direct technique for testing the applicability of Eqs. 12 and 13 because it tests in terms of the experimentally measurable parameter $F(t)$ and in terms of plots finally used in the analysis of FRAP data as described below.

The observations presented above can be used to evaluate $t_{1/2}$ values from experimental data by either nonlinear curve fitting of $F(t)$ vs. t with Eq. 12 or by a linear analysis of reciprocal plots. Both of these techniques use many points on the graph. A linear analysis has the advantage that it can be easily programmed into a minicomputer or performed with a hand calculator and provides a quick method for evaluating the large number of runs necessary to obtain good statistics when the FRAP technique is applied to living cells or tissues. Below we present the linear method of analysis that we use in the evaluation of FRAP data.

Because experimental reciprocal plots require a value of $F(\infty)$ they are subject to the experimental uncertainty in $F(\infty)$. This uncertainty, however, can be greatly reduced by the additional observation that a small error in the value of

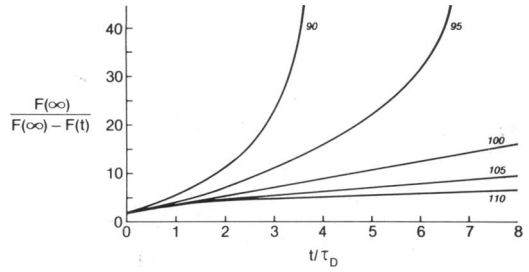

FIGURE 3 Graphs showing the effect of an error in the value of $F(\infty)$ on the linearity of a reciprocal plot. $F(t)$ vs. t was calculated with Eq. 1 for 50% bleach (K = 1.6) and a value of $F(\infty)$ equal to 100. The values of $F(t)$ were then used to calculate the graphs shown in this figure for several erroneous values of $F(\infty)$. The number next to each graph is the value of $F(\infty)$ used to calculate the reciprocal graph. Positive errors of a few percent in $F(\infty)$ cause upward deflections from a straight line while negative error causes downward deflections.

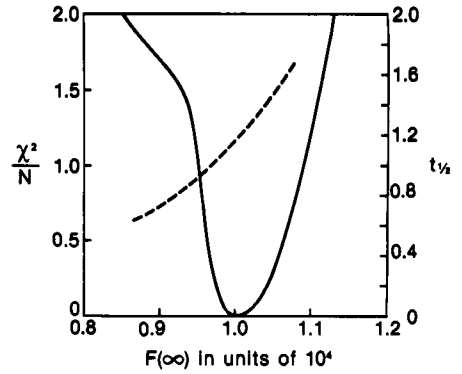

FIGURE 4 Graph demonstrating the effects of erroneous values of $F(\infty)$ on χ^2/N (solid line) and $t_{1/2}$ (dashed line). Intensity values used were calculated with Eq. 1 for 50% bleach (K = 1.6). The calculation was done with $F(\infty)$ 10,000 and $t_{1/2}$ = 1.16. The graphs show that χ^2/N minimizes at the correct values $F(\infty)$ = 10,000 and $t_{1/2}$ = 1.16.

$F(\infty)$ causes the reciprocal plot $R(t)$ vs. t to deviate significantly from linearity. This is demonstrated in Fig. 3, which shows that a small positive error of a few percent in $F(\infty)$ causes the plot to deviate upwards from a straight line while a small negative error causes a downward deviation. The correct value of $F(\infty)$ can thus be closely approximated by finding the value of $F(\infty)$ which gives the best straight line.

The exact method of analysis that we use is as follows. A value of $F(\infty)$ is estimated from the experimental graph of $F(t)$ vs. t and the experimental data is converted to $F(\infty)/F(\infty) - F(t)$ vs. t. The latter graph is then fitted to a straight line using the weighted method of least squares (12, p. 106). The closeness of fit of the straight line to the experimental data is measured in terms of reduced chi-square, χ^2/N, defined by the expression (12, p. 187):

$$\chi^2/N = [1/(N-2)] \sum_i^n W_i [R_i(t) - R_{ci}(t)]^2 \qquad (17)$$

where N is the number of experimental data points, $R_i(t)$ is the ith experimental data point, $R_{ci}(t)$ is the value of $R(t)$ calculated from the least-squares straight line through the points $R_i(t)$ and W_i is a weighting factor based on the error in $R_i(t)$. N-2 is the number of degrees of freedom for N data points fitted by a straight line. The value of $F(\infty)$ is then varied systematically and the value that minimizes χ^2/N is chosen as the best value of $F(\infty)$. The intercept and slope evaluated by the method of least squares with the best value of $F(\infty)$ is finally used to evaluate $t_{1/2}$ with Eq. 15.

The weighing function that we use is given by

$$W_i = \frac{[F(\infty) - F(t)]^4}{F(\infty)^2 F(t)}, \qquad (18)$$

which is based on the assumption that the experimental error in each data point is essentially due to counting error.

The manner in which χ^2/N and $t_{1/2}$ vary with errors in $F(\infty)$ is shown in Fig. 4. This figure was obtained by first generating values of $F(t)$ vs. t with Eq. 1, for the case $F(\infty)$ = 10,000, K = 1.60 (50% bleach) and $t_{1/2}$ = 1.16. Reciprocal plots for different values of $F(\infty)$ were then analyzed as described above. The nature of these plots is shown in Fig. 3. As can be seen from Fig. 4, χ^2/N minimizes at the correct value of $F(\infty)$, and the correct value of $t_{1/2}$ is obtained at the minimum of the graph.

The analysis as presented above yields best value of $F(\infty)$, $F(o)$, and $t_{1/2}$. It remains to show that the graph $\bar{F}(t)$ vs. t (see Eq. 7) calculated from experimental values of $F(t)$ and best values of $F(\infty)$ and $F(o)$ is indeed fitted by Eq. 1 with a value for τ_D calculated from the least-square value of $t_{1/2}$ and Eq. 8. In our experience, if the experimental graph of $R(t)$ gives a good fit to a straight line, then the graph $F(t)$ vs. t is always fitted by Eq. 1 with parameters derived from the straight line fit. It is nevertheless instructive to actually compare the experimental graph with the plot of $F_c(t)$ vs. t, where $F_c(t)$ is calculated with Eq. 1. To calculate $F_c(t)$ we must have values of K and β in addition to values for $F(o)$, $F(\infty)$, and $t_{1/2}$. Table I gives values for these parameters for different values of percent bleach. Experimental graphs of $F(t)$ are compared with graphs of $F_c(t)$ in the Results section.

Diffusion Plus Flow

Above we have considered the case where the recovery of fluorescence after bleaching is determined entirely by lateral diffusion. We now consider the effect of uniform flow or cell movement on the recovery $F(t)$ and reciprocal recovery $R(t)$ graphs. The interest here is how and to what extent flow can be detected in a FRAP experiment. As will be shown, reciprocal plots provide a convenient method for establishing the experimental precision needed to detect flow. The effect of flow on the recovery and reciprocal graphs is shown in Fig. 5 *a* and *b*. These graphs were calculated with Eqs. 7 and 9 for different ratios of τ_D:τ_F

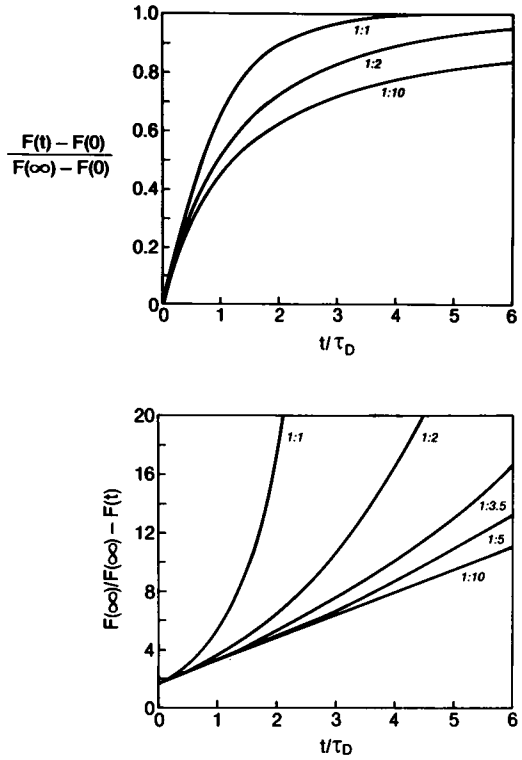

FIGURE 5 (*a*) Effect of flow on normalized recovery graphs. The graphs were calculated with Eqs. 5 and 7 for the case $K = 2$ (57% bleach). The ratio next to each graph represents ratio τ_D/τ_F. τ_D was held constant at 1.16. (*b*) Effect of flow on reciprocal recovery graphs. Graphs calculated for 57% bleach. Ratios next to graphs represent ratio τ_D/τ_F.

where τ_F, the characteristic time for recovery by flow, is defined in Eq. 10. The striking feature is that flow causes the reciprocal plots to deviate upwards from a straight line drawn through the initial points. In principle, flow can thus be detected as an upward curvature in the reciprocal plot. More precisely, our analysis indicates that if $F(\infty)$ is well known and intensity variations are due only to counting error, flow can be detected in reciprocal plots for values of $\tau_F/\tau_D \leq 2$.

In practice, the main limitations in detecting flow will be in the experimental precision for evaluating $F(\infty)$. An upward deviation from a straight line in an experimental reciprocal plot is not necessarily indicative of flow because, as shown above, a small percentage error in $F(\infty)$ causes a similar deviation in absence of flow. It is of interest then to determine whether our method for finding $F(\infty)$, by minimizing χ^2/N as described above, can also be used to distinguish between flow and an error in $F(\infty)$. More specifically, does the presence of flow make it impossible to linearize reciprocal graphs by adjusting the value of $F(\infty)$? To answer this question we have taken the graphs of Fig. 5 *a* for mixed flow and diffusion and treated them by our method to determine whether these plots can or cannot be linearized by an appropriate value of $F(\infty)$. The results indicate that for values of $\tau_F/\tau_D > 1.5$, it is indeed possible to find values of $F(\infty)$ that convert the reciprocal plots into straight lines within experimental errors. These conversions require values of $F(\infty)$ and $F(o)$ that are larger than the true values. The difference between true and adjusted values, however, is not large, <6%, and will be within experimental errors in most situations. For the case $\tau_F/\tau_D \sim 1$, it is still possible to find a value of $F(\infty)$ that linearizes the reciprocal plots, but the true and adjusted values for $F(\infty)$ will differ by >15%. This difference could probably be detected as an abnormally high value for $F(\infty)$ in the case of systems that display complete recovery of bleached intensity but may be difficult to detect for systems where the recovery is incomplete. In general, our analysis indicates that it would be difficult to detect flow for $\tau_F/\tau_D > 2$ and may be difficult to detect even for relative flow rates as high as $\tau_F/\tau_D \sim 1$.

It should be noted that when flow is present, its relative contribution to the recovery of fluorescence can be varied experimentally by varying the radius w. As shown in Eqs. 2 and 10, τ_D and τ_F are influenced differently by the value of w. The diffusion time, τ_D, is favored at small values of w while τ_F is favored at large value of w (5). Thus, if the presence of flow is suspected, the situation might be clarified by FRAP measurements at several values of w. Alternate methods for detecting flow by measurement of the intensity profile of the bleached area have been presented by other investigators (13, 14).

Two Diffusion Coefficients, Zero Flow

Finally we consider the case where the recovery of fluorescence involves two different molecules with diffusion coefficients D_1 and D_2. This situation arises, for example, when the fluorescent probe is bound to a molecule that exits in two different states of aggregation or to two molecular species with different diffusion coefficients. The interest here is to determine how much D_1 and D_2 must differ, to detect the presence of two different diffusion coefficients in a FRAP experiment. Fig. 6 shows reciprocal plots for

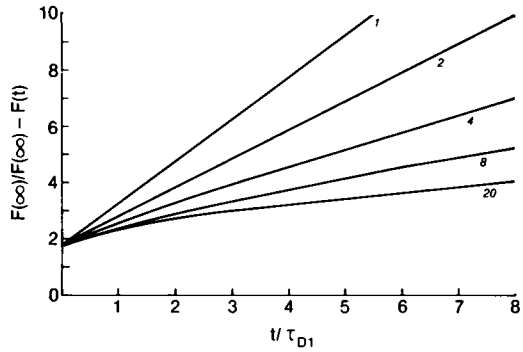

FIGURE 6 Graphs demonstrating the effect of two independent diffusion coefficients on reciprocal plots. The graphs were obtained by adding two equations of the form of Eq. 1, each with a different diffusion coefficient. The number next to each graph gives the ratio D_1/D_2. Graphs were calculated for 57% bleach. τ_{D1}, the characteristic diffusion time for the larger diffusion coefficient, was held at 1.16.

different values of D_1/D_2. We have assumed in this figure that each of the diffusing species contributes 50% to the total initial intensity and that each species is bleached by 50%. Data points were generated by adding two equations of the type shown in Eq. 1, each with a different diffusion coefficient. For values of $D_1/D_2 > 3$, the reciprocal plots are not linear, but in contrast to flow, see Fig. 6, the graphs bend downward. Therefore, in principle, the presence of two diffusion coefficients ($D_1/D_2 > 3$) can be detected in a reciprocal plot, as a deviation from linearity and distinguished from flow by a downward curvature. However, when $D_1/D_2 < 3$, the deviation from linearity is very small and would be undetectable in most experimental situations. An experimental reciprocal plot that is linear therefore may contain several diffusion coefficients whose values do not differ by more than a factor of three. In this case, the diffusion coefficient evaluated with Eqs. 8 and 15 represents an effective coefficient whose magnitude is determined by the separate diffusion coefficients and their fractional contributions to the recovery of fluorescence intensity.

The inability to resolve, in a given recovery graph, diffusion coefficients that differ by less than a factor of 3 should not be interpreted as indicating that small changes in the effective diffusion coefficient cannot be detected. On the contrary, it is possible experimentally to detect changes as small as 30% in the effective diffusion coefficient due to changes in the values of the diffusion coefficients and their fractional contributions to the recovery of fluorescence intensity. However, individual diffusion coefficients cannot be resolved.

Finally, it should be noted that, as in the case of flow, the ability to detect two diffusion coefficients for $D_1/D_2 > 3$ will be critically dependent on the experimental precision of $F(\infty)$.

EXPERIMENTAL METHODS

Thin, multibilayer films containing a fluorescent probe were formed from a chloroform solution of 40 mg/ml soybean lecithin (Sigma Chemical Co., St. Louis, MO, commerical grade) with 30% cholesterol and 3,3'-dihexyloxacarbocyanine iodide (Eastman Kodak Co., Rochester, NY) at a molar-lipid-to-probe ratio of 500:1. A thin film was formed by spreading 10 μl of the chloroform solution on a microscope cover glass, allowing most of the solution to roll off the cover glass, slowly evaporating the chloroform. The resulting thin, clear multibilayer film was hydrated by placing a small amount of fully hydrated agarose gel in contact with the edge of the film; the cover glass was sealed onto a microscope slide with a cavity.

The photobleaching apparatus was similar to that illustrated elsewhere (5) except that we used a helium/cadmium laser (Liconix, Sunnyvale, CA, model 410) having an output of 10 mW at 442 nm. The laser beam was focused onto a specific spot (1–3 μm diameter) of the multibilayer. Bleaching was achieved by removing an attenuator (1,000×) for 0.2 s.

RESULTS

Representative results in the form of reciprocal plots are shown in Fig. 7. The graphs in this figure were calculated

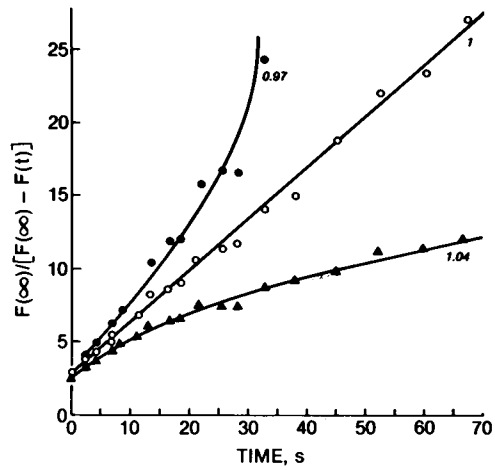

FIGURE 7 Reciprocal plots of experimental FRAP data from a multibilayer film of soybean lecithin with 30% cholesterol. The best values of $F(0)$, $F(\infty)$, and $t_{1/2}$ obtained by the procedure described in the text were 58.2×10^3, 93.4×10^3 and 7.4 s. Graph 1 was obtained using the best value of $F(\infty)$ and had a χ^2/N of 2.3. The other graphs were obtained by using values of $F(\infty)$ that were 0.97 and 1.04 of the best value of $F(\infty)$.

with data from a single recovery graph (32% bleach) using values for $F(\infty)$ that were 0.97, 1, and 1.04 of the best value. As previously described, the best value for $F(\infty)$ was determined by calculating reciprocal plots with different values of $F(\infty)$, fitting each plot to a straight line and calculating for each plot χ^2/N as defined in Eq. 17. The best value of $F(\infty)$ was selected as that which gave the minimum value of χ^2. Experimental plots of χ^2/N vs. $F(\infty)$, not shown, were found to display well-defined minima and to have the same shape as the theoretical graph in Fig. 4. Fig. 8 shows the normalized recovery graph and its fit by Eqs. 1, 5, and 6 using the best value for $F(0)$, $F(\infty)$, and $t_{1/2}$.

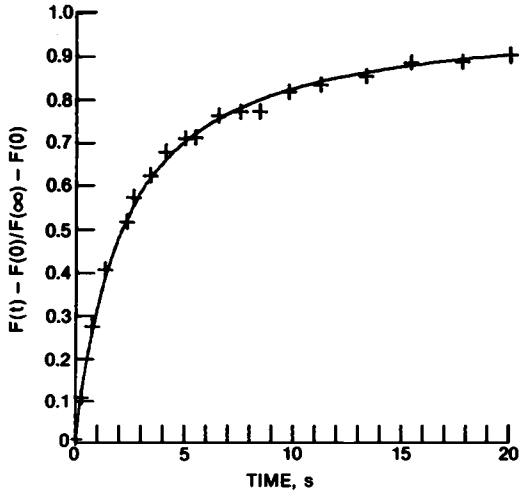

FIGURE 8 Normalized fractional recovery plot of the experimental data of Fig. 7. Crosses were calculated from experimental data using best values of $F(0)$ and $F(\infty)$. Solid graph was calculated with Eqs. 1, 7, and 8, using $t_{1/2}$ = 7.4 s, K = 0.94, and β = 1.1. Each unit on time scale corresponds to 3.38 s.

Values of χ^2/N from recovery graphs obtained over many days with multibilayers, as well as living cells, were in the range of 1.4 to 6. The value of χ^2/N for the data of Fig. 7 was 2.3. Visual inspection of the reciprocal plots showed that even for plots where the minimum χ^2/N was 6, the fit to a straight line was very good in the sense that the data points were randomly distributed about the least-square straight line. χ^2/N should be <1.5 if only counting errors are present (12, p. 190). The fact that we obtained values >1.5 indicates that counting error is not the only form of random noise present in some of our data.

Achievement of good agreement between experimental data and Eq. 1 requires careful adjustment of the FRAP instrumentation. In particular, the optics must be aligned to maintain as close to a Gaussian profile as possible at the image plane of the microscope objective. Moreover, care must be taken to assure that the bleaching beam coincides with the monitoring beam at the image plane of the microscope. This is often a serious problem in FRAP instruments where the bleaching pulse is produced by moving an optical attenuator. The movement produces small changes in the direction of the laser beam. In our system we have minimized this problem by using for the moveable attenuator a very thin glass plate which we coated with reflecting material. The short optical path-length minimizes displacement of the laser beam when the attenuator is moved. Thin Kodak plastic neutral density filters also minimize displacement but become partially bleached at powers >1 mW (beam diameter ~1 mm). These bleached filters greatly distort the Gaussian profile of the laser beam and often produce a fluorescent "spot" with a halo on a multibilayer or cell membrane. We have also found that chemical filters commonly used to attenuate laser beams are similarly bleached unless they are rapidly stirred.

The multibilayer films described above have proved to be useful not only in testing methods of analysis but also in aligning and focusing the laser beam. The very small thickness and high fluorescence intensity of the film allows the fluorescent "spot," produced by the laser beam at the image plane of the microscope objective, to be easily visualized and sharply focused with an external focusing lens. Moreover, when the multibilayer is unhydrated there is no recovery of fluorescence intensity for many hours after a bleaching pulse; that is, the film is permanently bleached for practical purposes. This allows the extent of coincidence of the bleached spot and the monitoring beam to be carefully evaluated. The multibilayer film also allows gross distortions of the beam profile at the image plane to be easily detected.

We have verified that the method of analysis presented here is applicable to FRAP data from biological cells and tissues and that living systems often yield recovery graphs that obey Eq. 1 when the optics are properly aligned and cell or tissue movement is eliminated.

Received for publication 7 April 1981 and in revised form 30 March 1982.

REFERENCES

1. Yguerabide, J. 1971. Abstract presented at the Biophysical Society meeting.
2. Peters, R. J., J. Peters, K. H. Tews, and W. Bahr. 1974. A microfluorimetric study of translational diffusion in erythrocyte membrane. *Biochim. Biophys. Acta.* 367:282–294.
3. Edidin, M., Y. Zagyansky, and T. J. Lardner. 1976. Measurement of membrane protein lateral diffusion in single cells. *Science (Wash., D. C.).* 191:466–468.
4. Koppel, D. E., D. Axelrod, J. Schlessinger, E. L. Elson, and W. W. Webb. 1976. Dynamics of fluorescence marker concentration as a probe of mobility. *Biophys. J. (Abstr.).* 16:216 *a.*
5. Axelrod, D., D. E. Koppel, J. Schlessinger, E. Elson, and W. W. Webb. 1976. Mobility measurement by analysis of fluorescence photobleaching recovery kinetics. *Biophys. J.* 16:1055–1089.
6. Jacobson, K., Z. Dersko, E. S. Wu, Y. Hou, and G. Poste. 1976. Measurement of the lateral mobility of cell surface components in single living cells by fluorescence recovery after photobleaching. *J. Supramol. Struct.* 5:565–576.
7. Barisas, B. G. 1980. Criticality of beam alignment in fluorescence photobleaching recovery experiments. *Biophys. J.* 29:545–548.
8. Barisas, B. G., and M. D. Leuther. 1979. Fluorescence photobleaching recovery measurement of protein absolute diffusion constants. *Biophys. Chem.* 10:221–229.
9. Woda, B. A., J. Yguerabide, and J. D. Feldman. 1980. The effect of local anesthetics on the lateral mobility of lymphocyte membrane proteins. *Exp. Cell Res.* 126:327–331.
10. Elson, H. F., and J. Yguerabide. 1979. Membrane dynamics of differentiating cultured embryonic chick skeletal muscle cells by fluorescence microscopy techniques. *J. Supramol. Struct.* 12:47–62.
11. Jesaitis, A. J., and J. Yguerabide. 1980. Lateral mobility of the $(Na^+\text{-}K^+)$-ATPase and a fluorescent lipid analog in the plasma membrane. Federation Proceedings Biophysical Society Meeting. *Fed. Proc. (Abstr.).* 39, (No. 6):1703.
12. Bevington, P. R. 1969. Data Reduction and Error Analysis for the Physical Sciences. McGraw-Hill Publications, New York. 106, 187, 190.
13. Smith, B. A., and H. M. McConnell. 1978. Determination of molecular motion in membranes using periodic pattern photobleaching. *Proc. Natl. Acad. Sci. U. S. A.* 75:2759–2763.
14. Koppel, D. E. 1979. Fluorescence redistribution after photobleaching: a new multipoint analysis of membrane translational dynamics. *Biophys. J.* 28:281–291.